(Received 31 December 2024, Accepted 16 March 2025, Scheduled 31 March 2025)

A Broadband Vertical Transition from Waveguide to Microstrip Based on Narrow-Wall Excitation

Jun Dong[1], Bingqing Zhong[1], Jing Zheng[1], Feng Yao[1], Jinxin Yin[1,*], and Hao Peng[2,*]

[1] College of Information Science and Engineering, Hunan Normal University, Changsha 410081, China
[2] School of Electronic Science and Engineering, University of Electronic Science and Technology of China, Chengdu 611731, China

ABSTRACT: In this paper, a broadband vertical rectangular waveguide (RWG)-to-microstrip line (MSL) transition structure for millimeter-wave solid-state circuits is proposed. The planar circuit in this transition is composed of a V-shaped probe and tapered fin-line ground, and the probe is inserted into the waveguide through a slot on the narrow side of the RWG. To facilitate energy coupling from RWG to MSL, a back-short with a length of a quarter-wavelength is designed on the bottom side of the probe to achieve effective electric coupling. A back-to-back prototype module has been designed to verify the performance of the transition. The measurement results show that the return loss of the back-to-back transition structure is better than 13 dB across the entire Ka-band, with the insertion loss (IL) of a single transition better than 0.55 dB. The measurement results agree well with simulation ones, validating the feasibility of the proposed transition circuit. A tolerance analysis is performed through simulations to verify the reliability of this transition design.

1. INTRODUCTION

In the context of the rapid evolution of communication technologies, the design and realization of high-performance millimeter-wave solid-state circuits have grown in significance. The millimeter-wave band, particularly Ka-band, is a key frequency range for achieving high-speed, high-capacity wireless communication due to its abundant spectrum resources [1, 2]. Metallic rectangular waveguides (RWGs), as the primary transmission medium for millimeter waves, offer advantages including high power capacity, high Q-factor, and low loss [3–5]. Meanwhile, microstrip line (MSL) is widely used in microwave and millimeter-wave planar integrated circuits due to its simple design, flexibility, and ease of integration with active components [6]. In modular millimeter-wave solid-state circuits, efficient transitions from RWG to MSL are critical for interconnecting test systems, feed networks, and integrated circuits. Therefore, achieving highly efficient RWG-to-MSL transitions is essential for the optimal performance of millimeter-wave solid-state circuits [7].

Among various RWG-to-MSL transition designs, vertical transitions have attracted significant attention due to their ability to effectively utilize vertical space, minimizing horizontal space usage [8–10]. Vertical RWG-to-MSL transitions typically achieve energy coupling through probe structures [11, 12], patches [13–16], or metal ridges [17], and are mostly fed through a slot on the broad side of the waveguide. However, this design is unsuitable for waveguide feed arrays that require multiple $\lambda/2$-spaced distances [18], as shown in Fig. 1. To overcome this limitation, a vertical RWG-to-MSL transition design based on narrow-wall feeding has been proposed [12–16]. This design allows for a more compact transverse feed port, addressing the issue of large transverse space usage in multi-array applications with broad-wall transitions. For the vertical RWG-to-MSL transition based on narrow-wall excitation, [12] presents a transition based on a folded MSL dipole radiating into the waveguide, achieving a 20% fractional bandwidth (FBW) in a back-to-back configuration. In [13], RWG is excited by a transverse patch antenna from a narrow-wall. To enhance bandwidth, an additional iris is inserted inside the waveguide. However, this design adds mechanical complexity, requires high-precision manufacturing, and the improved bandwidth is merely 15%. In [15], a transition based on the excitation of three overlapping transverse patches radiating into the waveguide's narrow-wall is designed, enabling both top-

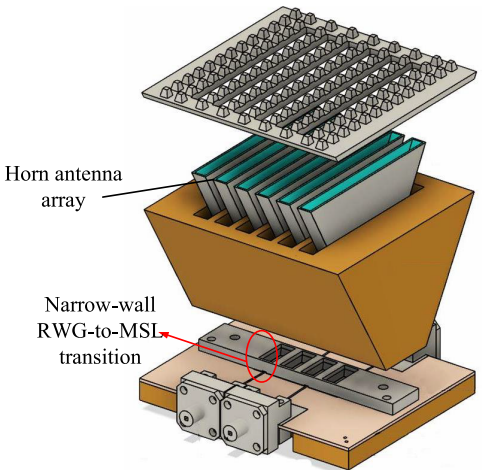

FIGURE 1. 3-D structure of horn antenna array based on narrow-wall RWG-to-MSL vertical transition feeding [18].

* Corresponding authors: Hao Peng (penghao@uestc.edu.cn); Jinxin Yin (yinjx02@126.com).

side and bottom-side feeding of the RWG-to-MSL transition. The top-side transition and bottom-side transition operate in Ka-band, providing 21.2% and 23% relative bandwidth, respectively. However, the bandwidth of the narrow-wall RWG-to-MSL transitions is still limited for broadband RF system application.

In this paper, a vertical narrow-wall RWG-to-MSL ultra-wideband transition structure based on fin-line ground and a V-shaped probe is designed, as shown in Fig. 2. The transition from the narrow-wall of RWG to MSL facilitates the compactness of the transverse excitation port for waveguide array antenna. The smooth transition between the probe and fin-line ground facilitates the transformation of the TE_{10} mode in the RWG to the quasi-TEM mode in the MSL. A back-short with a depth of a quarter-wavelength is designed below the probe to achieve effective electric field coupling. The proposed transition provides wideband performance without the need for additional iris structure inside the waveguide [11], simplifying the transition design and is suitable for antenna array based on narrow-wall feeding as shown in Fig. 1. A back-to-back transition model is verified, and measured results demonstrate that the proposed design achieves high-efficiency transition across the full Ka-band.

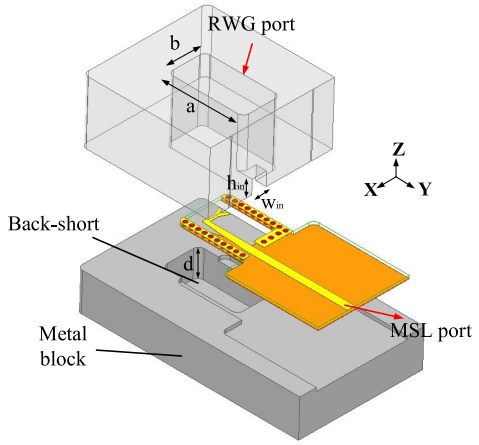

FIGURE 2. 3-D structure of the proposed RWG-to-MSL transition.

2. DESIGNS AND CONFIGURATION

2.1. Basic Configuration

The overall structure of the proposed vertical narrow-wall RWG-to-MSL transition based on the fin-line ground and V-shaped probe is shown in Fig. 2. The design concept is to couple the signal propagating in the vertical RWG to the horizontal MSL circuit plane while reducing transverse dimensions. As shown in Fig. 2, the transition structure consists of three parts: a standard RWG, a planar MS circuit, and a metal block with a back-short. The single-mode full-height WR-28 RWGs with dimensions of 7.112 mm × 3.556 mm and a frequency range from 26.5 GHz to 40 GHz have been designed. The right angles in the waveguides are rounded to 500-µm radius arcs to be compatible with the computer numerical control (CNC) milling process. The planar MSL circuit is designed on a 0.254 mm thick RT/Duroid 5880 substrate, as shown in Fig. 3. The substrate has a relative permittivity of 2.22 and a loss tangent of 0.009. The MSL circuit is inserted into the RWG, with the portion inside the waveguide including a tapered fin-line ground and a V-shaped probe to achieve field coupling and mode transition from TE_{10} to quasi-TEM. Via holes surround the aperture of the waveguide on the lower plane of the substrate to connect the surrounding ground and the waveguide short. The metal block not only provides mechanical support for the planar circuit but also functions as a reference short plane.

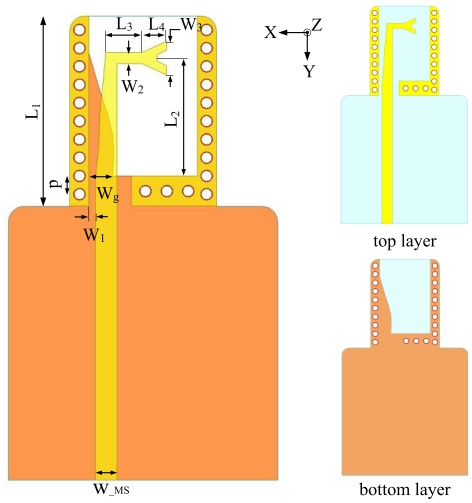

FIGURE 3. Geometry of the proposed planar circuit.

2.2. Electric Field Conversion

Figure 4 illustrates the progressive change of the electric field matching between the RWG and planar MSL circuit. The V-shaped probe, acting as a bridge connecting the RWG and MSL, is inspired by the probe, with a similar forked shape that has been used in broadband antenna propagation applications [19–21]. The majority of the coupled power is distributed along the edges of the probe and concentrated near the probe's base. As shown in Fig. 4, the transition process from RWG to MSL can be divided into several regions. In the RWG and Region A, only the dominant TE_{10} mode propagates within the single-mode RWG. When the signal is fed from the RWG into Region B-C, the two poles of the TE_{10} mode are sensed and coupled by the V-shaped probe and fin line ground, respectively. In Region B-C-D, the coupled electric field gradually rotates from the X-direction to Z-direction. Due to the gradual nature of the probe and fin line ground, the TE_{10} mode is progressively guided and transformed into the quasi-TEM mode.

2.3. Parameter Analysis

To improve impedance matching and achieve efficient coupling, a V-shaped probe is introduced at the termination of the MSL. Fig. 5 shows the simulation results of the L-shaped and V-shaped probes using the same method, which confirms the better performance of the V-shaped probe for the transition. As can be seen from the S-parameter results in Fig. 6, the proposed transition has two resonance points, which are mainly determined by the probe size (L_2) and back-short depth (d). L_2 is approximately half of the wavelength at the resonant frequency, while d is about a quarter-wavelength. Parameter sweeps of L_2

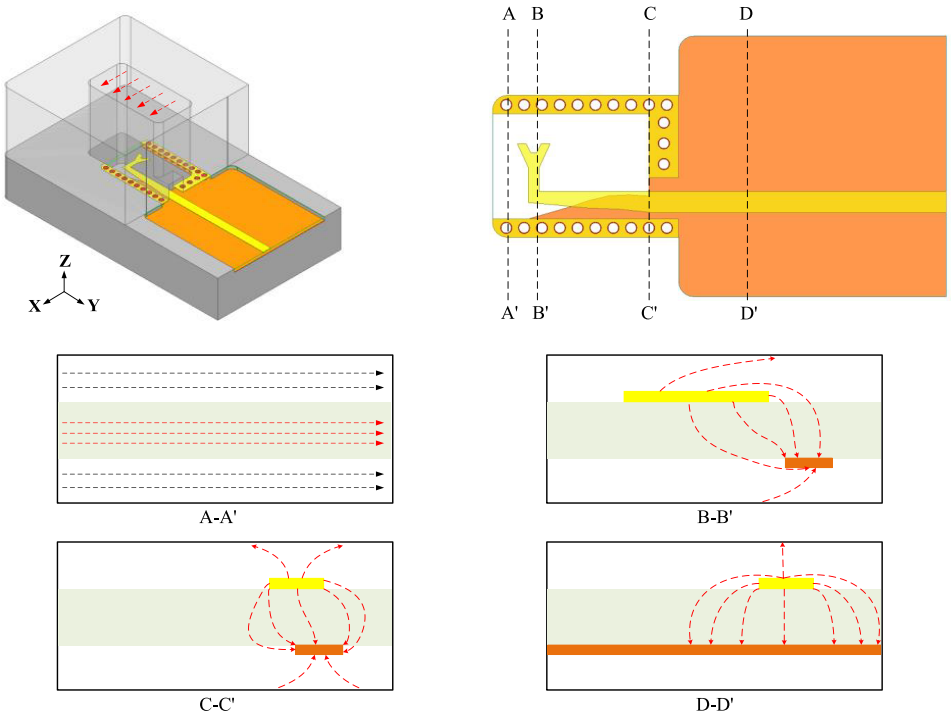

FIGURE 4. The transmission mode conversion process of the proposed narrow-wall RWG-to-MSL transition.

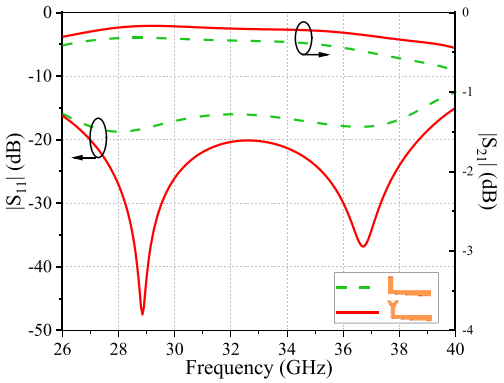

FIGURE 5. Comparison of transition performance between L-shaped probe and V-shaped probe.

and d are conducted, as shown in Figs. 6(a) and (b). The results indicate that the probe dimension L_2 mainly affects the second resonant frequency (around 37 GHz), and the lower resonant frequency is mainly affected by the back-short depth (d).

2.4. Assembly Sensitivity Investigation

To comprehensively investigate the performance of the proposed transition, the assembly sensitivity is analyzed through simulations. As shown in Figs. 7(a) and (b), the impact of the substrate offset by $\pm 10\%$ and $\pm 20\%$ from its original position in the X-axis and Z-axis directions, respectively, is analyzed. The results show that the return loss is still better than 15 dB in the operating frequency band, which indicates that the proposed transition has good assembly tolerance. The results demonstrate that the proposed transition has stable performance. The proposed transition circuit is simulated and optimized using 3D electromagnetic simulation software. The optimized parameters are listed in Table 1. The designed vertical transition achieves a return loss better than 15 dB across the frequency range of 26.5–40 GHz.

TABLE 1. Dimensions of the proposed RWG-MSL transition (unit: mm).

L_1	L_2	L_3	L_4	W_g
6.25	3.875	1.19	0.79	0.778
W_MS	W_1	W_2	W_3	p
0.72	0.208	0.37	1.1	0.6
a	b	h_{in}	W_{in}	d
7.112	3.556	1.3	1.4	2.24

3. RESULTS AND DISCUSSION

To experimentally validate the proposed design, two identical RWG-to-MSL transitions are cascaded in a back-to-back configuration. As shown in Fig. 8, a back-to-back transition prototype is fabricated. Measurements are conducted using a vector network analyzer (VNA). The measured results for the back-to-back transition are presented in Fig. 9, alongside the simulated results obtained using 3D electromagnetic simulation software. The measured data show that the return loss is better than 13 dB across the frequency range of 26.5–40 GHz. The insertion loss of the back-to-back transition, including the loss from an 18 mm microstrip transmission line, ranges from 0.6 to 1.1 dB over the 26.5–40 GHz frequency band. This indicates that the insertion loss for a single transition is less than 0.55 dB.

Table 2 summarizes the proposed transition with the published vertical narrow-wall RWG-to-MSL transitions for com-

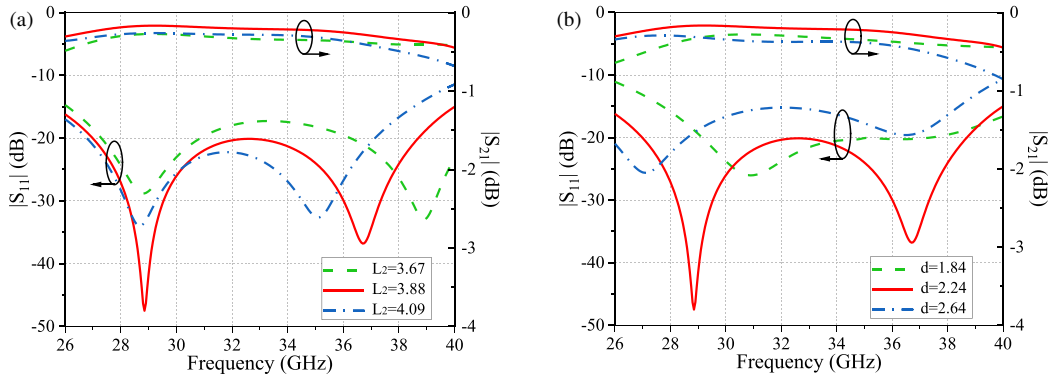

FIGURE 6. Parametric study of the proposed transition. (a) Probe dimension L_2. (b) Back-short depth d.

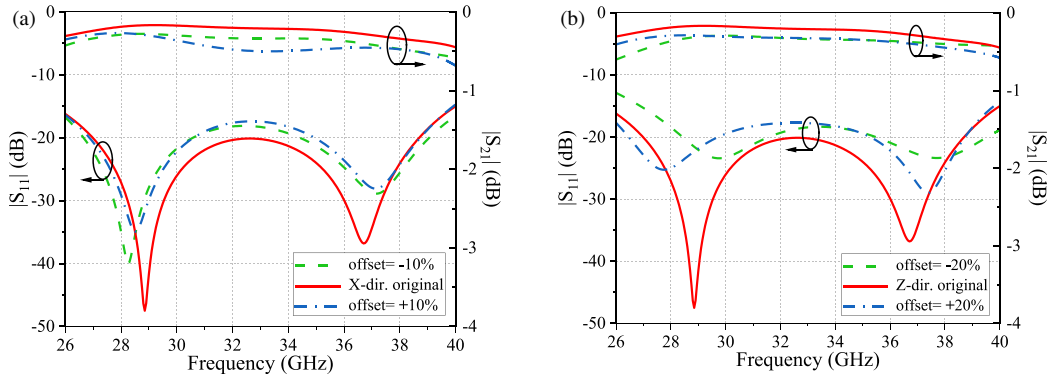

FIGURE 7. Simulated results of the proposed transition with different substrate position offset value. (a) X-axis direction. (b) Z-axis direction.

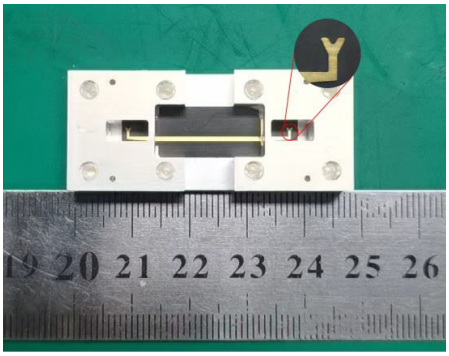

FIGURE 8. Photograph of the fabricated back-to-back transition.

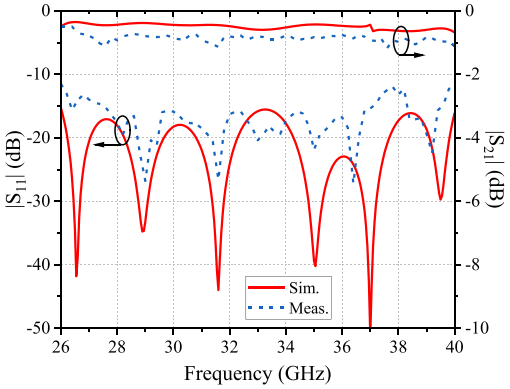

FIGURE 9. The cross section of the PMa-BSynRM.

TABLE 2. Comparison with the existing vertical narrow-wall RWG-to-MSL transitions.

Reference	Frequency	Bandwidth	Return Loss	Max. IL	Structure
[12]	72.75–89.5 GHz	20%	$>$ 10 dB	1.7 dB	microstrip folded dipole
[13]	76–88 GHz	15%	$>$ 10 dB	1.2 dB	coplanar patch antenna, inductive waveguide iris
[14]	86–91.2 GHz	6%	$>$ 15 dB	6 dB	patch with a parasitic element
[15]	24.6–31 GHz	23%	$>$ 10 dB	1.7 dB	overlapped patches
[16]	74.9–78 GHz	4.1%	$>$ 15 dB	1 dB	V-shaped patch
This work	26.5–40 GHz	40.6%	$>$ 13 dB	1.1 dB	V-shaped probe and fin-line ground

parison. It is noted that those measured results are based on back-to-back transitions. In [14], the dielectric is loaded in the waveguide, resulting in high insertion loss. It can be seen that the proposed transition achieves a wider operating bandwidth than the transitions presented in [12–16] while maintaining the comparable assembly complexity.

4. CONCLUSION

A vertical narrow-wall waveguide-to-microstrip transition based on a V-shaped probe and fin-line ground is proposed and verified. The proposed transition has been validated in the Ka-band by fabricating a back-to-back transition prototype. Reasonable agreement is obtained between the simulated and measured results. This transition exhibits a wider operating bandwidth, easy assembly, and improved assembly tolerance, which is suitable for waveguide antenna array fed from the narrow-wall of waveguide.

ACKNOWLEDGEMENT

This work is supported by Humanities and Social Sciences Research Program Youth Fund Project of the Ministry of Education of China under Grant No. 20YJCZH020, YueLuShan Center Industrial Innovation of Hunan, China under Grant No. 2023YCII0107, National Students' Platform for Innovation and Entrepreneurship Training Program under Grant No. 202210542067, the Fundamental Research Funds for the General Program of National Natural Science Foundation of China under Grant No. 62471092.

REFERENCES

[1] Thompson, J., X. Ge, H.-C. Wu, R. Irmer, H. Jiang, G. Fettweis, and S. Alamouti, "5G wireless communication systems: Prospects and challenges [guest editorial]," *IEEE Communications Magazine*, Vol. 52, No. 2, 62–64, 2014.

[2] Gupta, A. and R. K. Jha, "A survey of 5G network: Architecture and emerging technologies," *IEEE Access*, Vol. 3, 1206–1232, 2015.

[3] Deslandes, D. and K. Wu, "Integrated microstrip and rectangular waveguide in planar form," *IEEE Microwave and Wireless Components Letters*, Vol. 11, No. 2, 68–70, 2001.

[4] Mottonen, V. S. and A. V. Raisanen, "Novel wide-band coplanar waveguide-to-rectangular waveguide transition," *IEEE Transactions on Microwave Theory and Techniques*, Vol. 52, No. 8, 1836–1842, 2004.

[5] Dong, Y., T. K. Johansen, V. Zhurbenko, and P. J. Hanberg, "Rectangular waveguide-to-coplanar waveguide transitions at U-band using *E*-plane probe and wire bonding," in *2016 46th European Microwave Conference (EuMC)*, 5–8, London, UK, 2016.

[6] Gao, Y., F. Zhang, Y. Qiao, J. Zang, L. Li, and X. Shang, "A microstrip filter direct-coupled amplifier based on active coupling matrix synthesis," *Frontiers of Information Technology & Electronic Engineering*, Vol. 22, No. 9, 1260–1269, 2021.

[7] Hafeez-Ur-Rehman, Ha Il Song, Sean Park, and Jae-Hyung Jang, "Broadband partially covered microstrip-to-waveguide transition with enhanced radiation suppression for millimeter-wave transmission," *IEEE Microwave and Wireless Technology Letters*, Vol. 34, No. 4, 367–370, 2024.

[8] Xu, Z., J. Xu, and C. Qian, "Novel in-line microstrip-to-waveguide transition based on *E*-plane probe T-junction structure," *IEEE Microwave and Wireless Components Letters*, Vol. 31, No. 9, 1051–1054, 2021.

[9] Hannachi, C., T. Djerafi, and S. O. Tatu, "Broadband *E*-band WR12 to microstrip line transition using a ridge structure on high-permittivity thin-film material," *IEEE Microwave and Wireless Components Letters*, Vol. 28, No. 7, 552–554, 2018.

[10] Zhang, B., H. Zhu, and Y. Zhang, "Wideband in-line waveguide-to-microstrip transition with antisymmetric rectangular probes," *IEEE Microwave and Wireless Technology Letters*, Vol. 34, No. 6, 591–594, 2024.

[11] Zhang, B., Y. Zhang, C. Wu, and T. Cao, "Millimeter-wave broadband waveguide-to-microstrip transition using a bifurcated probe," *IEEE Microwave and Wireless Components Letters*, Vol. 32, No. 9, 1031–1034, 2022.

[12] Zhou, I. and J. Romeu, "Ultrawideband microstrip to waveguide transition for 5G millimeterwave applications," in *2022 16th European Conference on Antennas and Propagation (EuCAP)*, 1–4, Madrid, Spain, 2022.

[13] Topak, E., J. Hasch, and T. Zwick, "Compact topside millimeter-wave waveguide-to-microstrip transitions," *IEEE Microwave and Wireless Components Letters*, Vol. 23, No. 12, 641–643, 2013.

[14] Häseker, J. S. and M. Schneider, "90 degree microstrip to rectangular dielectric waveguide transition in the W-band," *IEEE Microwave and Wireless Components Letters*, Vol. 26, No. 6, 416–418, 2016.

[15] Zhou, I. and J. R. Robert, "Ultra-wideband narrow wall waveguide-to-microstrip transition using overlapped patches," *Sensors*, Vol. 22, No. 8, 2964, 2022.

[16] Seo, K., K. Sakakibara, and N. Kikuma, "Narrow-wall-connected microstrip-to-waveguide transition using V-shaped patch element in millimeter-wave band," *IEICE Transactions on Communications*, Vol. 93, No. 10, 2523–2530, 2010.

[17] Deutschmann, B. and A. F. Jacob, "A full W-band waveguide-to-differential microstrip transition," in *2019 IEEE MTT-S International Microwave Symposium (IMS)*, 335–338, Boston, MA, USA, 2019.

[18] Zhou, I., L. Pradell, J. M. Villegas, N. Vidal, M. Albert, L. Jofre, and J. Romeu, "Microstrip-fed 3D-printed H-sectorial horn phased array," *Sensors*, Vol. 22, No. 14, 5329, 2022.

[19] Klemm, M., I. Z. Kovcs, G. F. Pedersen, and G. Troster, "Novel small-size directional antenna for UWB WBAN/WPAN applications," *IEEE Transactions on Antennas and Propagation*, Vol. 53, No. 12, 3884–3896, 2005.

[20] Xu, L., Z.-Y. Xin, and J. He, "A compact triple-band fork-shaped antenna for WLAN/WiMAX applications," *Progress In Electromagnetics Research Letters*, Vol. 40, 61–69, 2013.

[21] Pradnyana, K. D., D. Wijoyono, G. Adriandi, and F. Y. Zulkifli, "Modified Y-shape patch ultra-wide band monopole antenna," in *TENCON 2017 — 2017 IEEE Region 10 Conference*, 1620–1623, Penang, Malaysia, 2017.